

CEBAF



0205 9100 002 728 4

**LARGE ACCEPTANCE DETECTORS
FOR ELECTROMAGNETIC NUCLEAR PHYSICS**

V.D. Burkert and B.A. Mecking

Physics Division
Continuous Electron Beam Accelerator Facility
Newport News, Virginia 23606, USA

ABSTRACT

The physics program and the requirements for large acceptance detectors in electromagnetic nuclear physics are discussed. As a specific example, the CEBAF Large Acceptance Spectrometer is presented.

To appear as a chapter in the book
Modern Topics in Electron Scattering
Edited by B. Frois and I. Sick
World Scientific, Singapore

LARGE ACCEPTANCE DETECTORS FOR ELECTROMAGNETIC NUCLEAR PHYSICS

V.D. Burkert and B.A. Mecking

Physics Division
Continuous Electron Beam Accelerator Facility
Newport News, Virginia 23606, USA

ABSTRACT

The physics program and the requirements for large acceptance detectors in electromagnetic nuclear physics are discussed. As a specific example, the CEBAF Large Acceptance Spectrometer is presented.

A. INTRODUCTION

Electron scattering experiments have provided most of our knowledge of the structure of nucleons and nuclei. The standard experimental equipment at electron accelerators consists of focusing magnetic spectrometers to detect the scattered electron (sometimes in coincidence with a second charged particle). The main advantage of these spectrometers is the high resolution (that relies on the use of carefully arranged magnetic fields) and the low sensitivity of the particle detector system to background (the detectors are located in a well shielded enclosure far away from both target and beam). The disadvantage, however, is the small acceptance in both solid angle and momentum which limits the experiments in practice to the coincident detection of two (perhaps, in selected cases, three) particles. A further drawback is the massive iron structure which limits the minimum angle between the detected particles and makes a continuous coverage of the available phase space impossible. For the coincident detection of several particles in the final state, the ideal solution is a detector capable of covering the complete solid angle and momentum range of interest for all outgoing charged and neutral particles.

Large acceptance detectors have been routinely used in combination with tagged bremsstrahlung photon beams. In this case, the instantaneous photon beam intensity is limited by accidental coincidences to $\sim 10^7$ sec resulting in relatively low background rates. Recent examples for large acceptance detector systems are TAGX¹ at the Tokyo synchrotron and SAPHIR² at the Bonn synchrotron (both using a transverse field dipole as the analyzing element).

Very few large acceptance detectors have been employed in fixed target electron scattering experiments. These were aimed at studies of pion and vector meson production, in particular at the Cornell, DESY, and Bonn electron synchrotrons. In the following section, some relevant parameters of these experiments are listed.

1. The DESY Streamer Chamber Experiment.

At the DESY 7.2 GeV electron synchrotron a streamer chamber located in a the gap of a large dipole magnet was used³ to measure the channel $ep \rightarrow e\pi^+\pi^-p$. The necessity to measure four charged particle in the final state afforded use of a large acceptance detector with nearly 4π solid angle. A sketch of the apparatus is shown in Figure 1. The primary electron beam penetrated the active volume of the streamer chamber. The $2 \mu\text{sec}$ memory time of the streamer chamber limited the number of incident electrons during the spill time of the beam to about $4 \cdot 10^7$ per second. With a 9 cm long liquid hydrogen target, this corresponds to an instantaneous luminosity (target density \cdot beam intensity) of $L = 1.5 \cdot 10^{31} \text{ cm}^{-2}\text{sec}^{-1}$.

2. The Cornell LAME Experiment.

The LAME set-up at the Cornell 12 GeV electron synchrotron used a large transverse field dipole magnet⁴. Particles were detected in proportional chambers (located in the magnet gap) with a total of 22,000 sense wires. The primary electron beam passed through an insensitive region of the proportional chambers (Figure 2). Despite considerable problems caused by forward going electrons being spread out by the transverse field ('sheet of flame'), the spectrometer operated at instantaneous rates of 10^9 electrons/sec on a 7.5 cm long liquid hydrogen target corresponding to a luminosity of $3.2 \cdot 10^{32} \text{ cm}^{-2}\text{sec}^{-1}$.

3. The Bonn Large Acceptance Spectrometer.

A group working at the 2.5 GeV electron synchrotron of the Bonn university⁶ used a magnetic spectrometer with a large opening at forward angles, allowing the simultaneous detection of electrons and protons in an angular range of 5° to 14° . The apparatus is shown in Figure 3. For the momentum analysis a large dipole

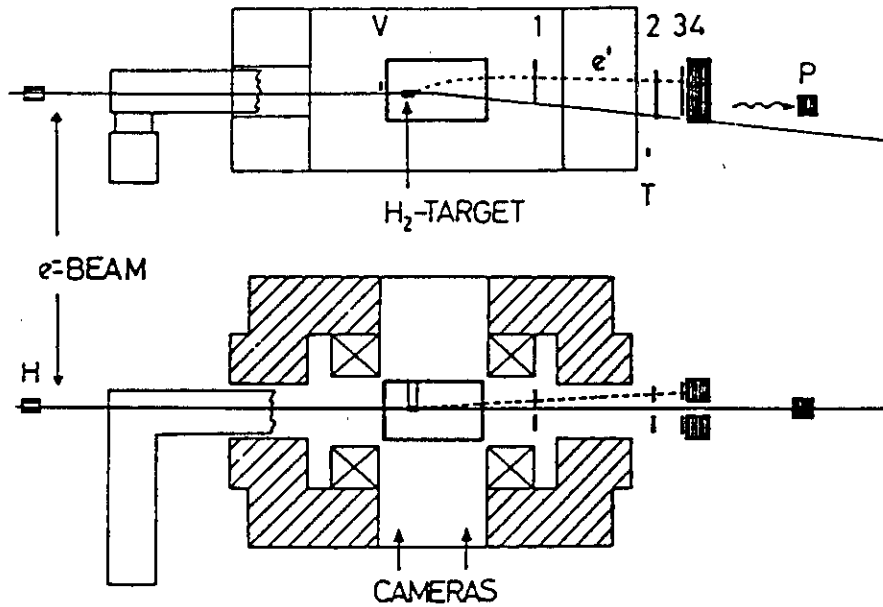


Figure 1. Sketch of the streamer chamber experiment used at DESY to study multiple pion electroproduction.

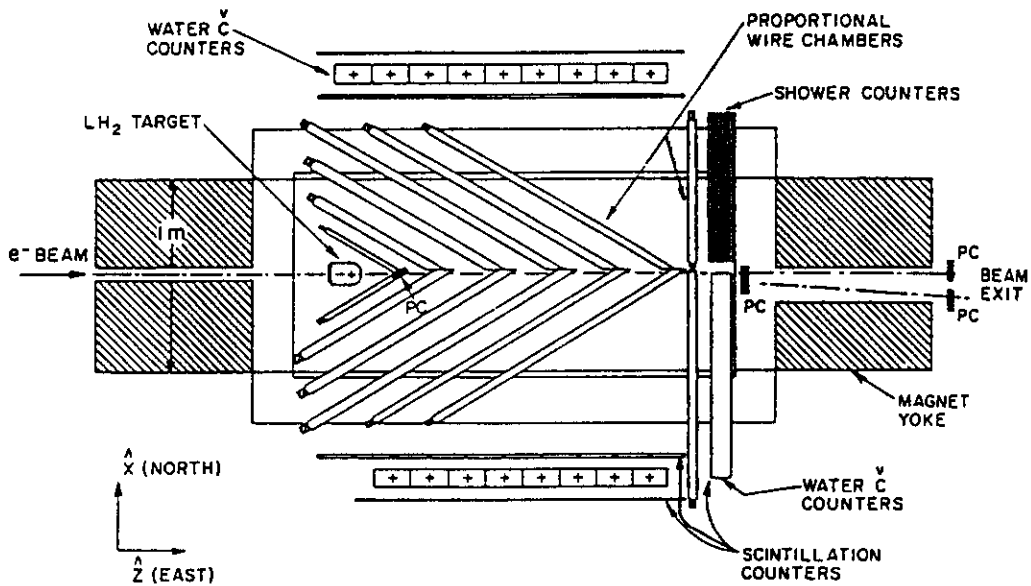


Figure 2. The Cornell LAME apparatus was used to study the electroproduction of vector mesons⁵.

Lab	E (GeV)	$\Delta\Omega(\text{sr})$	$\frac{\delta P}{P}$ (FWHM)	$L(\text{cm}^{-2}\text{s}^{-1})$	$\bar{L}(\text{cm}^{-2}\text{s}^{-1})$
DESY	7	$\sim 3\pi$	$4 \cdot 10^{-3} \cdot P$	$1.5 \cdot 10^{31}$	$1.5 \cdot 10^{30}$
Cornell	12	$\sim 2.5\pi$	$2 \cdot 10^{-2} \cdot P$	$3.2 \cdot 10^{32}$	$3.2 \cdot 10^{31}$
Bonn	2	0.5	$3 \cdot 10^{-2}$	$1.8 \cdot 10^{34}$	$6 \cdot 10^{32}$

To operate a large acceptance detector at the highest possible luminosity, a high quality electron beam with 100% duty-cycle is advantageous. Most experiments, which make use of solid or liquid targets, require relatively low electron currents. However, high intensity is required for thin target experiments, especially for polarized gas targets.

At electron accelerators with 100% duty-cycle the data rates in large acceptance detectors are, to a large degree, not limited by the luminosity achievable, but rather by the collection speed of the data acquisition system. It is interesting to note that this eliminates the traditional 'rate advantage' of hadronic reactions over electromagnetic processes. Electromagnetic reactions may hence be studied with statistical sensitivity similar to hadronic reactions. This brings to bear the full capability of the electromagnetic interaction as a probe of the internal structure of hadrons and nuclei.

B. PHYSICS PROGRAM FOR A LARGE ACCEPTANCE DETECTOR

Experimental programs that require a large acceptance detector (LAD) can be divided into the following categories:

1. measurements where the detection of multiple particle final states is required
2. measurements at limited luminosity. The limitation can be due to the target or due to the beam.
3. measurements with high background rejection requirements. For the coincident measurement of n uncorrelated particles, the ratio of the number of signal to noise events (S/N) is given by:

$$\frac{S}{N} = K \cdot \left[\frac{1}{\text{luminosity}} \cdot \frac{\text{duty - cycle}}{\text{time resolution}} \cdot \frac{\text{target length}}{\text{vertex resolution}} \right]^{n-1}$$

where K is a factor which is specific to the reaction studied. Experiments requiring a large S/N ratio often need to reduce the luminosity. The loss in count rate must then be compensated by an increase in solid angle acceptance if the other parameters are kept constant.

4. measurements requiring high relative accuracy under changes in the experimental conditions.

The following sections gives four examples for physics programs that will need or benefit from these capabilities: electromagnetic production of N^* resonances, hyperon production, multi-nucleon emission in electro- induced processes, and the study of the Drell-Hearn Gerasimov sum rule.

Electromagnetic Excitation of Baryon Resonances

An important goal of intermediate energy nuclear and particle physics is to obtain a fundamental understanding of the strong interaction and the structure of baryons. Many important experiments have been carried out for the proton because of its easy accessibility as a target. However, the ultimate goal is unlikely to be reached from looking solely at the ground state of the nucleon system.

Based on our detailed understanding of QED, the study of electromagnetic excitation of nucleon resonances will allow the testing of wave functions for the excited states. In the simplest picture each baryon has 3 quarks in shell-model orbitals. The nucleon has all quarks in relative s-states, and excited states are created by raising the quarks to excited orbitals. The correct model is probably much more complicated, but it must have similar basic features. The interaction of the baryon constituents, quarks and gluons, is generally believed to be described by QCD, the theory of strong interactions. However, solutions of this theory in the non-perturbative domain are extremely difficult to achieve. The lattice gauge theory offers the best hope for exact calculations, but results seem to be far in the future. Thus, models which contain QCD ingredients in simplified, presently calculable form will continue to play an important role. Microscopic models, such as dynamical quark models, bag models, and QCD sum rules, relate the internal baryon structure to the strong interaction of the confined constituents. Probing baryons with photons and electrons will give us insight into this fundamental

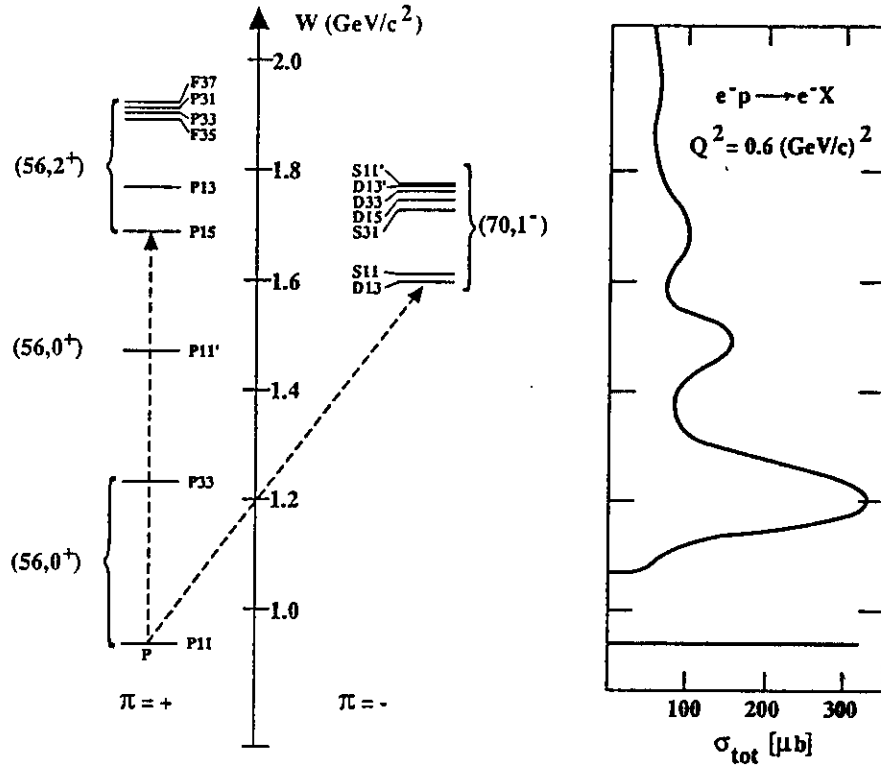


Figure 4. The experimentally known non-strange baryon states with masses $\leq 2 \text{ GeV}/c^2$ (left), and the shape of the total photoabsorption cross section at $Q^2 = 0.6 (\text{GeV}/c)^2$ (right).

interaction⁸. This is the main thrust of experiments using the electromagnetic probe.

In the total photo-absorption cross section for inclusive electron scattering off proton targets ($eN \rightarrow e'X$) (see Figure 4) broad bumps are seen with a smooth underlying background, clearly indicating the excitation of resonances in the mass range below $2 \text{ GeV}/c^2$. The states all have strong decay channels, giving widths of 100 - 250 MeV which prevents separating them in inclusive measurements. However, the decay into meson-nucleon states have characteristic branching ratios and angular distributions which can be measured in exclusive experiments (e.g. $ep \rightarrow ep\pi^0$ or $ep \rightarrow ep\pi^+\pi^-$). These data allow identification of the quantum numbers of the intermediate state. Many of the lower lying resonances ($W \leq 1.8 \text{ GeV}$) decay strongly into the $N\pi$ or $N\eta$ channel and are therefore most accessible through single π and η production processes. Such experimental studies will involve measurements of single pseudoscalar meson production employing unpolar-

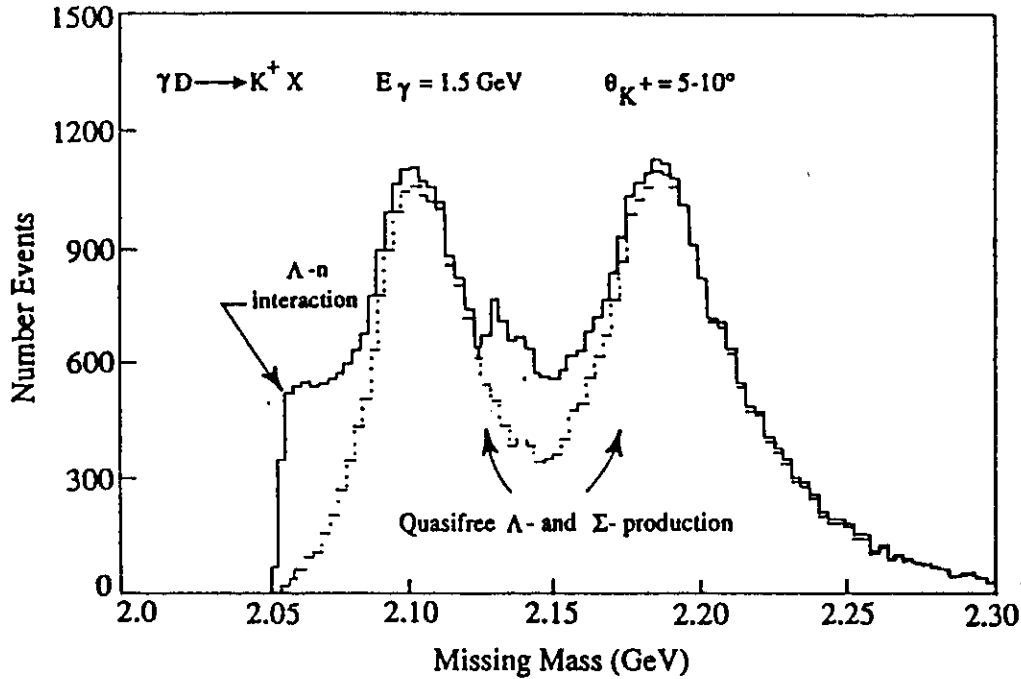


Figure 5. Monte Carlo simulation of the process $\gamma D \rightarrow K^+ X$. The cusp near 2.13 GeV is due to the $N\Sigma$ threshold. The cross section near the Λn threshold is sensitive to the Λn final state interaction.

ized beams and targets, as well as polarized beams, polarized targets and possibly recoil polarimetry. In some cases, in particular for resonances in the higher mass region, the $N\rho$, $\Delta\pi$ channels leading to $\pi\pi N$ final states, and the $N\omega$ channel are also very sensitive to resonance excitation.

A large acceptance detector is ideally suited to carry out this experimental program. Because of the large acceptance, all reaction channels, even those involving multi-pion final states, can be studied simultaneously. To disentangle the spin and isospin structure of the states, measurements using polarized electrons and polarized proton and deuterium targets have to be performed.

Hyperon Production

The study of systems with a strange quark, especially the photo- and electro-production of hyperons both in elementary and nuclear processes, will add to our understanding of fundamental two-particle interactions and will provide an

opportunity to test and extend models developed for NN and πN interactions.

When a hyperon is embedded in a nuclear system, it can be viewed as a controlled impurity which, in contrast to nucleons, is not restricted by the Pauli principle. It also lives long enough to sample its hadronic environment. Therefore, it can probe the deep interior of the nucleus.

To interpret the hypernuclear data, the elementary production amplitudes have to be known. The first step is a measurement of the production cross section for $K^+\Lambda$ and $K^+\Sigma$ off the proton combined with a measurement of the hyperon polarization. The next logical step is the investigation of these reactions in the few-body system. Ultimately, one would like to study the properties of nuclear systems that contain a bound hyperon⁹.

To give an example, kaon production on deuterium can be used to investigate the following questions (Figure 5):

- o In quasifree kinematics, the differential cross section for the elementary reaction $\gamma n \rightarrow K^+\Sigma^-$ can be determined from a measurement of the $K^+\pi^-$ -neutron final state.
- o Λn and $\Sigma^0 n$ final state interactions can be studied by going away from quasifree kinematics.
- o $\Lambda - \Sigma$ channel coupling effects are predicted to lead to a cusp effect as the threshold for Σ^- production is crossed.
- o In the vicinity of the Σ^- cusp, theoretical predictions can be tested by searching for strangeness -1 dibaryons.

Kaons can be produced by tagged bremsstrahlung photons via the $\gamma N \rightarrow KY$ reaction and detected in a LAD. The mass of the hyperon-nucleon system can be determined by combining the energy of the incident photon and the outgoing kaon. The angular distribution of coincident hadrons from the decay of the hyperon-nucleon system allows a determination of the final state hyperon polarization.

Multi-Nucleon Emission

Several areas of physics may be studied by using electromagnetic multi-nucleon knockout reactions. These areas include three-body currents, meson exchange currents, nucleon-nucleon ground state correlations, and multi-quark clusters. A LAD is ideally suited for the experimental study of these reactions.

To date, two-nucleon knockout and higher multiplicity studies have not seriously been attempted. This is due to the lack of both high quality electron accelerators (high energy, high duty-cycle) and large acceptance spectrometers. Cross sections for two-nucleon knockout are of order $\text{pb}\cdot(\text{sr}\cdot\text{MeV})^{-3}$; hence counting rates are low. High luminosity experiments using small solid angle detectors have unacceptable accidental coincidence rates. A LAD in combination with a high duty-cycle electron accelerator will be ideally suited for this type of work. Operating a LAD at a luminosity of $10^{34}\text{cm}^{-2}\text{s}^{-1}$ yields typical count rates for specific multi-nucleon kinematics of 10-100 events/hr with negligible contributions due to accidental coincidences. Much of the physics of interest occurs in the continuum where moderate momentum resolution is sufficient.

The large acceptance permits the simultaneous measurement of cross sections over a large kinematic range. For example, at an incident electron beam energy of 2 GeV, the range in momentum and energy transfer is $Q^2=(0.1 - 1.0) (\text{GeV}/c)^2$ and $\nu = (0.05 - 1.0) \text{GeV}$ on a ^3He target.

The large acceptance also provides the capability for out-of-plane measurements. These measurements are useful in understanding the physics of scattering processes. A classic example consists of the longitudinal-transverse and transverse-transverse interference terms in the single particle production cross section which depend on $\cos 2\phi$ and $\cos\phi$, respectively:

$$\frac{d\sigma}{d\Omega} = \sigma_T + \epsilon\sigma_L + \epsilon\sigma_{TT}\cos 2\phi + \sqrt{2\epsilon(1+\epsilon)}\sigma_{TL}\cos\phi \quad (1)$$

Thus the study of cross sections as a function of the azimuthal angle ϕ around the momentum transfer vector provides a tool for separately determining those components of the cross section which are of interest while suppressing others which constitute background.

Drell-Hearn Gerasimov (DHG) Sum Rule

The results of the polarized proton structure functions measurement by the EMC collaboration¹⁰ has generated new interest in experimental tests of the famous sum rule of Drell, Hearn¹¹ and Gerasimov¹². The sum rule relates the difference in the total photo-absorption cross section on nucleons for photon-nucleon helicity $\lambda_{\gamma N} = 1/2$ and $\lambda_{\gamma N} = 3/2$ to the anomalous magnetic moment of the target nucleon:

$$\int_{\nu_{th}}^{\infty} \frac{d\nu}{\nu} [\sigma_{1/2}(\nu, 0) - \sigma_{3/2}(\nu, 0)] = -\frac{2\pi^2\alpha}{M^2} k^2 \quad (2)$$

where ν is the photon energy, $\sigma_{1/2}$ and $\sigma_{3/2}$ are the absorption cross sections for total helicity 1/2 and 3/2, and k is the anomalous magnetic moment of the target

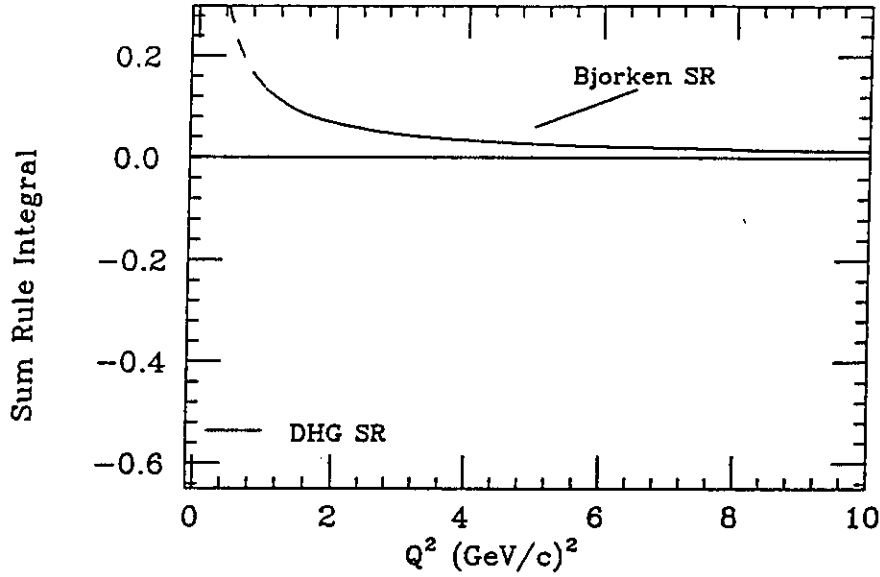


Figure 6. Q^2 - dependence of the Bjorken sum rule for protons, as suggested by data on the polarized proton structure functions¹⁴. The arrow indicates the prediction of the DHG sum rule at $Q^2 = 0$.

nucleon. The interpretation of the EMC results on the polarized proton structure functions in terms of the Bjorken sum rule¹³ suggests¹⁴

$$\int_{\nu_{thr}}^{\infty} \frac{d\nu}{\nu} [\sigma_{1/2}(\nu, Q^2) - \sigma_{3/2}(\nu, Q^2)] \simeq \frac{0.2}{Q^2} \cdot \frac{8\pi^2 \alpha}{M^2} \quad (3)$$

The latter sum rule should be valid in the deep inelastic region. A comparison of (2) and (3) suggests that dramatic changes in the helicity structure of the γp coupling must occur when going from the deep inelastic region to $Q^2 = 0$, if the DHG sum rule were to be fulfilled. This is illustrated in Figure 6. The DHG sum rule has been derived on rather general grounds but has never been tested experimentally. An analysis of single pion production experiments places some limits on how much this sum rule may be violated¹⁵. By using a circularly polarized tagged photon beam and a polarized proton target (e.g. $N\bar{H}_3$), the total absorption cross section difference $\sigma_{1/2} - \sigma_{3/2}$ can directly be measured as a function of the photon energy. A LAD allows measurement of the total photo-absorption cross section by measuring at least one of the photoproduced particles. The integral in (2) is weighted by $1/\nu$, therefore the lower energy regime gives important contributions. Medium energy machines and LAD's are therefore appropriate instruments for testing this sum rule.

C. REQUIREMENTS AND DESIGN CHOICES FOR LAD'S

To carry out a broad physics program of the type outlined before, a general purpose large acceptance spectrometer with the following properties will be required:

1. Homogeneous coverage of a large angular and momentum range for charged particles, photons, and neutrons:

- angular range for particle detection $5^\circ \leq \Theta \leq 150^\circ$
- momentum range for charged particles $p \geq 100 \text{ MeV}/c$
- energy range for photons $E \geq 50 \text{ MeV}$

2. Good momentum and angular resolution:

- momentum resolution (small Θ , high p) $\delta p/p \simeq 0.5\%$ (FWHM)
- momentum resolution (large Θ , low p) $\delta p/p \simeq 1.0\%$ (FWHM)
- angular resolution $\delta\Theta \simeq 1.0 \text{ mrad}$

Due to the Lorentz-boost, the average particle momentum increases with decreasing emission angle. In order to keep the absolute momentum resolution constant, the relative $\delta p/p$ has to improve in the forward direction.

3. Good particle identification: separation of electrons, pions, kaons, protons and deuterons in the momentum range of interest.

4. High luminosity and count rate capability. The spectrometer should be able to operate in the difficult background environment encountered in electron scattering experiments. Design goals are:

- electron beam luminosity $L \simeq 10^{34} \text{ cm}^{-2} \text{ sec}^{-1}$
- photon beam intensity $N \leq 10^8 / \text{sec}$

Fast detector elements and a high level of segmentation are required. To control the large flux of particles from electromagnetic processes, the magnetic field configuration should have the following features:

- o deflect low-momentum charged particles at large angles and keep them away from the tracking detectors. The largest contribution

comes from electrons which are elastically scattered off atomic electrons (Moller scattering)

- o not deflect forward-going charged particles (like electrons that lost energy due to bremsstrahlung or e^+e^- -pairs generated from conversions of bremsstrahlung photons) into the detector. Consequently, transverse magnetic field components at the beam axis should be avoided.

The requirements 1-4 listed above are indispensable for practically all experimental programs. The following properties 5 and 6 are vital for specific experiments:

5. The spectrometer should allow operation of polarized targets (solid state or gaseous) requiring their own magnetic guiding field or other complicated equipment in the target region (cryogenic or track sensitive targets, vertex detectors etc.). Therefore, sufficient space (e.g. ~ 1 meter diameter for polarized solid state targets) in the target region is required. The magnetic field of the spectrometer should vanish in the target region to avoid interference with the polarized target field.

6. Open geometry for the installation of detectors with a long flight path for neutron detection.

The operation of the spectrometer (e.g. triggering) and the data analysis (e.g. pattern recognition and the determination of the track parameters) will be facilitated by the following properties:

7. Symmetry around the beam axis

8. Homogeneous magnetic field

The consequences of the requirements outlined above for the choice of the magnetic field configuration have been studied. Solenoids with longitudinal field, dipoles with transverse field, and toroidal magnets with the axis along the beam line have been considered. In all cases, the target has been assumed to be inside the magnetic field volume. The configurations will be discussed in more detail.

Solenoid

Solenoids have become the standard magnet configuration for large acceptance spectrometers at e^+e^- - and $p\bar{p}$ - colliders. Solenoids offer large solid angle coverage, high tolerance to backgrounds and efficient pattern recognition and tra-

Table 2: Desirable Features of a Large Acceptance Detector for Electromagnetic Nuclear Physics		
Feature		Importance for Physics Program
Angular range		
θ	5° - 160°	**
ϕ	0° - 360°	*
Momentum range [GeV/c]	≥ 0.1	**
Momentum resolution (FWHM)		
small θ , high p	$\leq 0.5\%$	***
large θ , low p	$\approx 1.0\%$	***
Particle identification	perfect	**
Maximum luminosity [$\text{cm}^{-2} \text{s}^{-1}$]	10^{34}	***
Magnetic field at target location (for polarized target operation)	0	**
Mechanical structure (neutron ToF)	open	*
Trajectory reconstruction	simple	*

jectory reconstruction. Momentum resolution at large angles with respect to the solenoid axis can be very good. At small angles, however, the outgoing particles move essentially in the direction of the magnetic field and experience only a small deflection. This results in poor momentum resolution at small angles. For e^+e^- - collider applications, the loss in momentum resolution at small angles can be tolerated since the laboratory system coincides with the center-of-mass system.

Dipole

Dipole magnets have been used for electroproduction experiments, especially at high energies (≤ 10 GeV). In the forward direction, they can achieve good ϕ - coverage and high momentum resolution. Disadvantages are the limited ϕ - coverage at large scattering angles and the sensitivity to charged electromagnetic background which is spread out by the transverse field.

Polarized solid state targets are very difficult to accommodate in both solenoid

Table 3: Advantages and Drawbacks of Toroidal Magnetic Spectrometers

Feature	Advantage	Drawback
Magnetic field always transverse to particle trajectory	efficient use of installed B field, particle tracks at different ϕ don't mix	need independent detection system for each segment + large number of detector elements
Coils can be shaped to give desired $\int Bdl$ as a function of θ	improved $\delta p/p$ for high p, forward going particles + can account for Lorentz boost	inhomogeneous magnetic field, complicated trajectory reconstruction, ϕ -coverage limited by coils
Efficient coverage of large field volume	good momentum resolution, good particle identification via ToF	expensive calorimetry due to large surface area
Field-free region around the target and the beam line	space for polarized target, no interference with polarized target magnetic field	low energy background can travel long distances + first detector far away from the target + limited accuracy for vertex reconstruction
Open mechanical structure	flexibility to add detectors outside + long time-of-flight path for neutrons possible	

Table 4: Comparison of Magnetic Field Configurations for Large Acceptance Detectors			
Feature	Solenoid	Dipole	Toroid
Solid angle coverage			
θ -range	+	+	++
ϕ -range	+++	--	-
Momentum range	++	++	++
Momentum resolution			
small θ , high p	--	++	++
large θ , low p	++	++	++
Particle identification	+	++	++
High electron beam luminosity	++	-	++
Polarized target operation	--	-	++
Open structure for neutron ToF	--	+	++
Simple trajectory reconstruction	++	-	--

and dipole spectrometers because of their large size and their high magnetic fields. Only for those experiments where coverage of the forward part of the solid angle is sufficient, can the problem be solved by putting the target upstream of the detector.

Toroid

Toroidal magnet spectrometers offer a field-free region around the target and a magnetic field that is always transverse to the particle momentum (important for high momentum resolution). Since the ϕ -pattern of the event is preserved, the determination of ϕ is decoupled from the measurement of polar angle Θ and momentum p. These properties of toroidal spectrometers have often captured the imagination of physicists, especially in the planning stage for a new accelerator. The main disadvantages of toroidal spectrometers are the lack of complete ϕ -coverage due to the coils and the inhomogeneous magnetic field which makes trajectory reconstruction more complicated than in a uniform field. Table 3 lists advantages and drawbacks of toroidal spectrometers.

None of the magnetic field configurations can satisfy all requirements. Table 4 lists advantages and disadvantages (designated by + and - signs) of the choices considered. The best choice depends on the details of the physics program.

D. THE CEBAF LARGE ACCEPTANCE SPECTROMETER

Based on the previous discussion, the toroidal configuration seems to be the best choice for the CEBAF physics program*. Therefore, the CEBAF Large Acceptance Spectrometer (CLAS) is designed as a magnetic toroidal multi-gap spectrometer. The magnetic field is generated by six super-conducting coils arranged around the beam line to produce a magnetic field which is primarily in the ϕ -direction. A perspective view of the spectrometer magnet is shown in Figure 7. A top view of the particle detection system is given in Figure 8, a view in the direction of the beam (cut in the target region) in Figure 9. The detection system consists of drift chambers to determine the track of charged particles, gas Čerenkov counters for electron identification, scintillation counters for the trigger and for measuring time-of-flight, and an electromagnetic calorimeter to detect showering particles like electrons and photons. The segments are individually instrumented to form six independent magnetic spectrometers. This will facilitate pattern recognition and track reconstruction at high luminosity.

Charged particles are tracked by drift chambers whose wires are arranged in 3 regions: Region 1 close to the target, Region 2 between the coils, and Region 3 outside of the coils. Each drift chamber region defines a track segment independent of the other regions. The combination of axial wires oriented perpendicular to the beam axis, and stereo wires oriented at 6° with respect to the axial wires allow a complete geometric reconstruction of charged tracks. The distribution of energy loss in the drift cells is recorded and provides additional information for particle identification. For electron scattering experiments, a small normal-conducting toroid surrounding the target will be used to keep low momentum charged background from reaching the Region 1 drift chamber.

The threshold gas Čerenkov counters are sensitive to particles with $\beta \geq 0.998$. In combination with the electromagnetic calorimeter they give good electron identification, sufficient even at large electron scattering angles where the π/e ratio becomes large. The location of the Čerenkov counters in front of the scintillation counters minimizes photon conversion and knock-on electrons.

The scintillation counters serve the double purpose of contributing to the first level trigger and providing time-of-flight information. Each counter is viewed by

* Similar conclusions were reached by physicists working at the MIT Bates Linear Accelerator. They are presently designing an 8 coil toroid for internal target experiments at the Bates South Hall Ring.

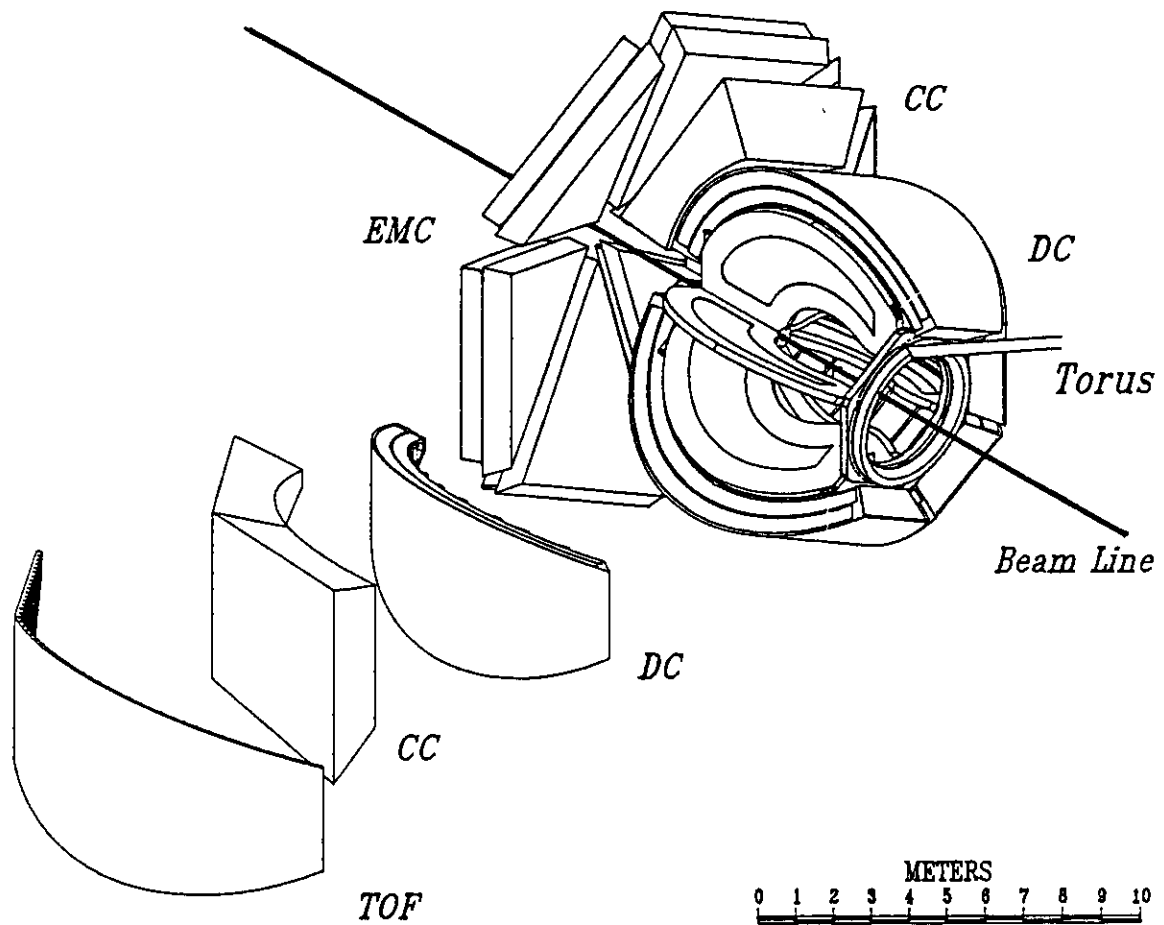


Figure 7. *The CEBAF Large Acceptance Spectrometer. Six symmetrically arranged superconducting coils generate an approximate toroidal magnetic field. Drift chambers (DC), time-of-flight counters (TOF), gas Čerenkov counters (CC), and electromagnetic calorimeters (EMC) provide particle identification, charged particle tracking, and energy measurements for electromagnetic particles. A field-free region around the target allows use of polarized gas and solid state targets.*

phototubes at both ends for improved timing and position resolution. A single counter covers the full ϕ -range corresponding to one segment, but a Θ -range of only $\sim 3^\circ$. This facilitates the selection of kinematical quantities, e.g. the electron

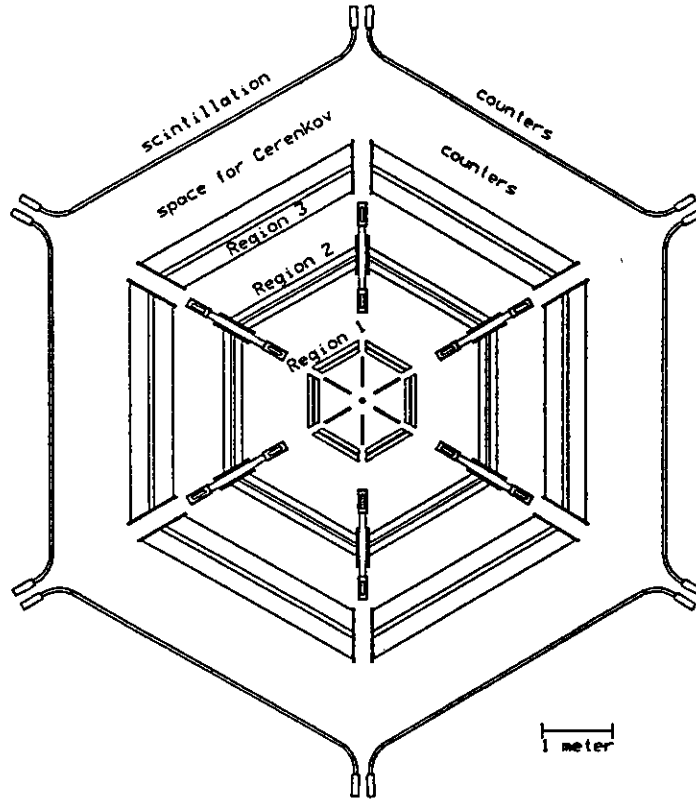


Figure 8. *Transverse cut through the CLAS magnet and detector system at the target location. Each of the three drift chamber regions consists of six axial layers and six layers of stereo wires tilted by 6° with respect to the axial wires. In the transverse view, particle trajectories are approximately straight lines.*

scattering angle, in the trigger.

The electromagnetic calorimeter is used for the identification of electrons and the detection of photons from the decay of hadrons, such as π^0 , η , η' , and Λ^* . The calorimeter allows an energy measurement for electromagnetic particles with $\sigma_E/E \leq 0.1/\sqrt{E(\text{GeV})}$ and provides ≤ 10 mrad for the angular resolution. This allows the reconstruction of π^0 events from their 2γ decay with an invariant mass resolution of $\delta m/m \leq 0.15$, sufficient to allow separation of π^0 , η , and η' events. The calorimeter is made of alternating layers of lead sheets as showering material and plastic scintillator strips. The scintillator strips in subsequent layers are rotated by 120° to provide stereo information needed for unambiguous multihit recognition.

Ideally, the solid angle covered by Čerenkov counters and electromagnetic calorimeters should be complete. Initially, electron detection will be provided up to 45° in all 6 segments.

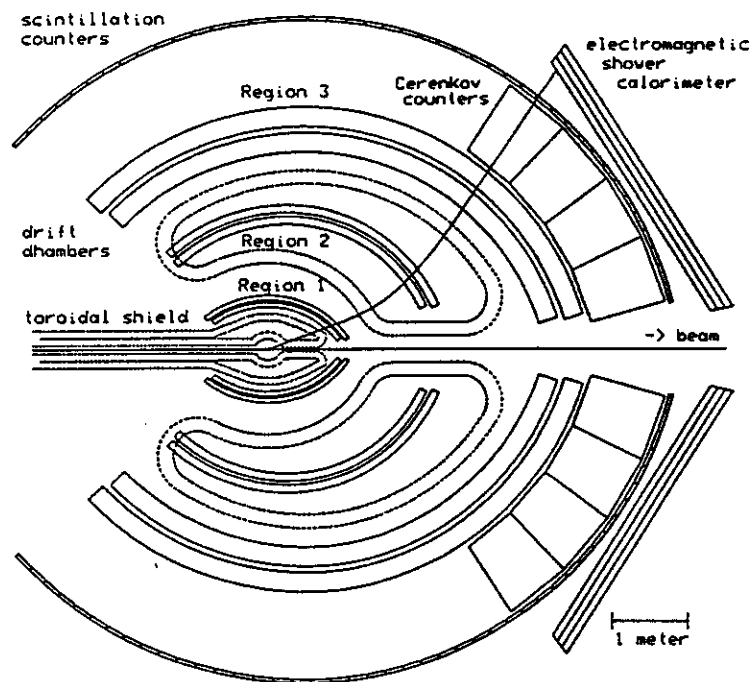


Figure 9. Cut through the CLAS detector system along the beam axis. The forward angles (up to $\Theta = 45^\circ$) are covered by gas Čerenkov counters and electromagnetic calorimeters. Particle tracking and time-of-flight measurements are available over most of the angular range.

Expected Performance of CLAS

The CLAS will be located in CEBAF's hall B. A bremsstrahlung tagging spectrometer is located in an enlarged tunnel section at the entrance of the hall. For tagged photon experiments, the primary electron beam will be deflected vertically into a low-power beam dump. Equipment to monitor the tagged photon beam, e.g. a pair spectrometer, will be located in an enlarged downstream tunnel section. A polarimeter to measure the polarization of the incident electron beam will be located in the upstream beam tunnel. The hall and the beam dump are fully shielded to allow for experiments that use a high-intensity beam on a thin target (e.g. polarized ^3He gas target)

For electron scattering experiments, the small normal conducting toroidal shielding magnet is an essential element of the apparatus. This is demonstrated in Figure 10, where the effect of this magnetic shield on the electromagnetic background load of the region 1 drift chamber for hydrogen targets is shown. A reduction of the background load by two orders of magnitude is achieved by an

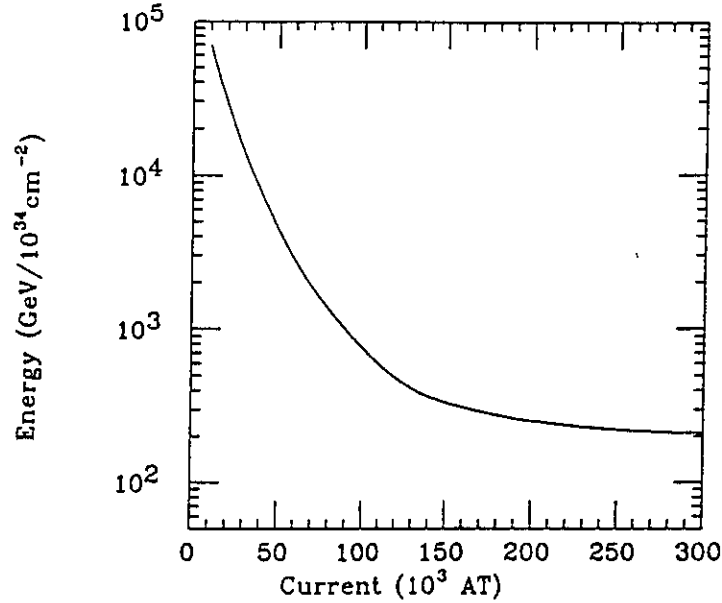


Figure 10. Electromagnetic background load in the region 1 drift chamber system as a function of the current in the normal conducting toroidal shielding coils for a 10 cm long hydrogen target. The energy deposition for an integrated luminosity of 10^{34} cm^{-2} is displayed.

appropriate magnetic field. The remaining background is due to low energy photons from direct or secondary electromagnetic processes. For light nuclear targets the situation is similar to hydrogen. However, for high Z targets the background is largely composed of X-rays emitted from the target after electron knock-out due to Moller scattering. This contribution reduces the maximum luminosity to values of about $10^{33} \text{ cm}^{-2} \text{ sec}^{-1}$.

The proposed physics program for CLAS makes use of the identification of neutral particles in exclusive reactions such as:

$$ep \rightarrow ep\pi^0, e\eta, e\pi^+n$$

or

$$\gamma p \rightarrow K^+\Lambda, K^+\Sigma^0, K^+\Lambda^*$$

using the missing mass technique. In Figures 11 and 12, the expected resolution in the mass of the undetected system is shown for the processes $ep \rightarrow epX$ and $\gamma p \rightarrow K^+X$. The expected resolution allows the separation of the exclusive channels which are of interest. Direct measurement of π^0 and η particles emitted at forward angles can be accomplished by measuring their 2γ decays using the electromagnetic calorimeter. Figure 13 shows the expected invariant mass resolution for 1.5 GeV/c π^0 events. Identification of π^0 , η , and η' will be possible.

Table 5 summarizes the expected performance of the CLAS detector.

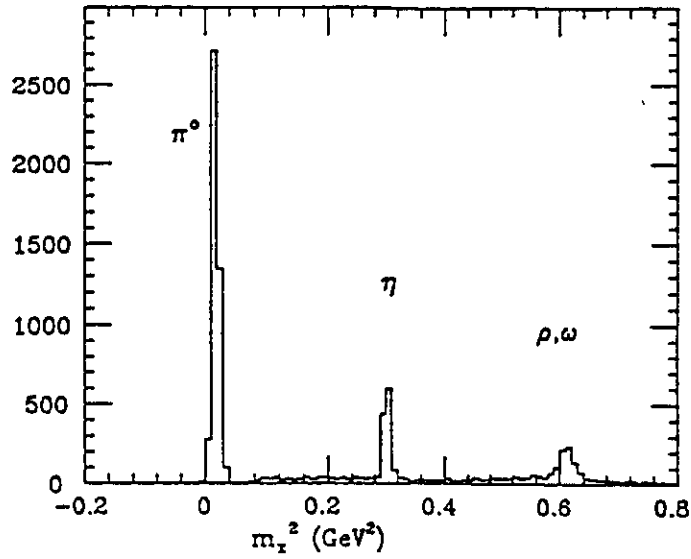


Figure 11. Monte Carlo simulation of the process $ep \rightarrow epX$ in the nucleon resonance region. The π^0 , η , and $\omega - \rho$ peaks can be identified.

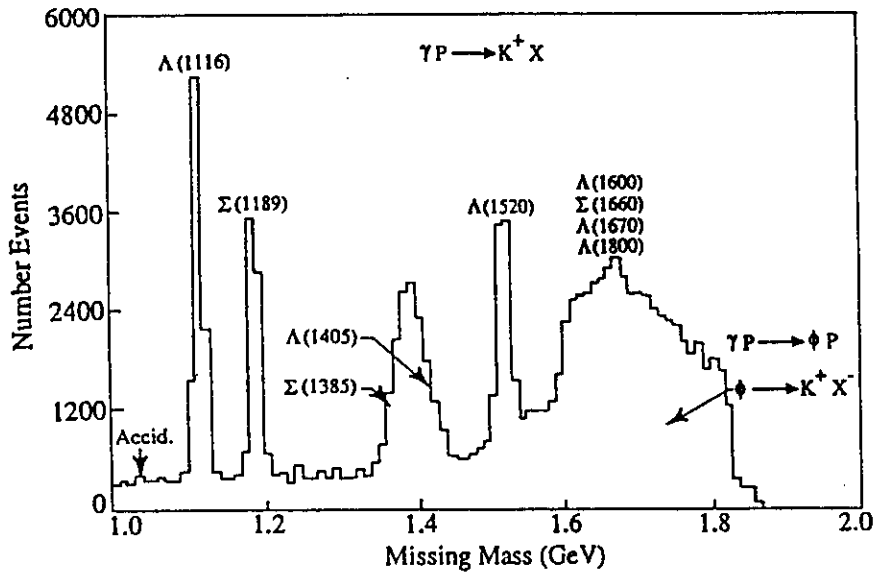


Figure 12. Monte Carlo simulation of the process $\gamma p \rightarrow K^+ X$ for 2.5 GeV photons. The ground state hyperons and the $\Lambda^*(1520)$ excited state can be uniquely identified.

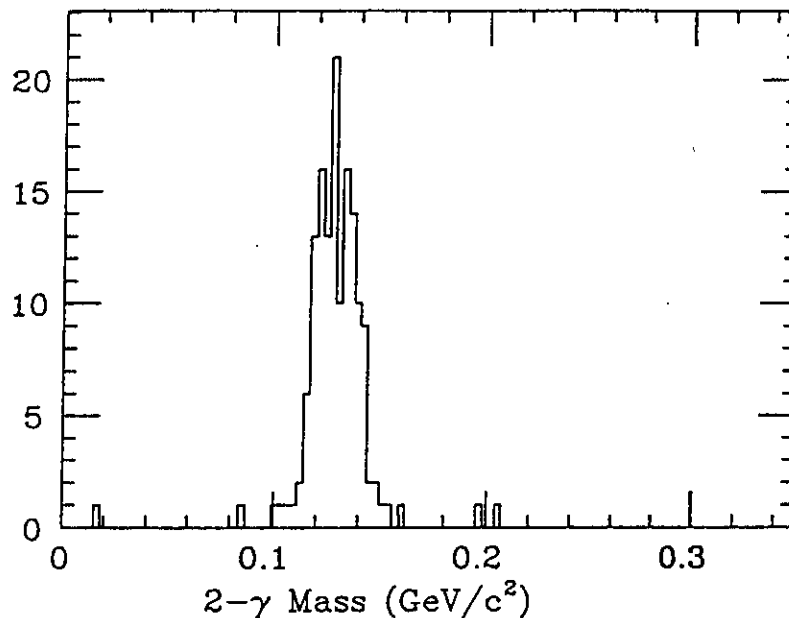


Figure 13. Monte Carlo simulation and invariant mass reconstruction of $\pi^0 \rightarrow \gamma\gamma$ events in the CLAS electromagnetic calorimeter.

E. SUMMARY AND OUTLOOK

A large class of physics problems, ranging from studies of the elementary excitation of the nucleon to the electromagnetic response of heavy nuclei, will benefit from large acceptance detectors capable of detecting both the scattered electron and the coincident hadrons in the same device.

As demonstrated using the CEBAF Large Acceptance Spectrometer as an example, the physics requirements can be essentially met making use of the technical progress in particle detectors.

Open detector systems can only tolerate a limited instantaneous background rate. The optimum environment for the operation of large acceptance detectors is provided by an electron beam with 100% duty-cycle. The advent of these accelerators can therefore be expected to provide a dramatic boost for the physics output derived from large acceptance detectors

Table 5: CEBAF Large Acceptance Spectrometer CLAS Expected Performance	
θ -acceptance	$8^\circ - 140^\circ$
ϕ -acceptance $\theta = 10^\circ$ $\theta = 20^\circ$ $\theta = 90^\circ$	50 % of 2π 65 % of 2π 85 % of 2π
Momentum range $\theta = 20^\circ$ (outbending tracks) $\theta = 20^\circ$ (inbending tracks) $\theta = 90^\circ$	≥ 0.2 GeV/c ≥ 1.5 GeV/c ≥ 0.1 GeV/c
Momentum resolution (FWHM) $\theta = 20^\circ, p = 4$ GeV/c $\theta = 90^\circ, p = 1$ GeV/c	≤ 0.5 % ≈ 1.0 %
Particle identification (ToF + dE/dx) maximum momentum for separation of π/K π/proton K/proton	2.0 GeV/c 3.0 GeV/c 3.5 GeV/c
Maximum luminosity	$10^{34} \text{ cm}^{-2} \text{ s}^{-1}$
Magnetic field (within a 20 cm radius around the target)	≤ 1 G

REFERENCES

- [1] K. Niki, et al., Nucl. Instr. Meth. A294, 534 (1990)
- [2] R.J. Wedemeyer, Lecture Notes in Physics 234, 392 (1985)
- [3] V. Eckardt et al., Nuclear Physics B55 (1973) 45-82.
- [4] L.A. Ahrens et al., Nucl. Instr. Meth. 173 (1980) 537.

- [5] D.G. Cassel, Proc. CEBAF Summer Workshop, Newport News, Virginia, eds: F. Gross and R. Whitney, pg. 104 (1985).
- [6] H. Blume et al., Z. Phys. C 16, 283 (1983)
- [7] For an overview see: G. Gidal, B. Armstrong, and A. Rittenberg, Lawrence Berkeley Laboratory Report LBL-91, supplement, revised (1985)
- [8] For an overview see: Proc. Workshop on 'Excited Baryons 1988', Troy, NY, 4-6 August, 1988, eds: G. Adams, N.C. Mukhopadhyay, P. Stoler, published by World Scientific.
- [9] For an overview see: C.B. Dover, Nucl. Phys. A450, 95 (1987); M.P. Locher et al., Adv. Nucl. Phys. 17, 47 (1987)
- [10] J. Ashman, et al., Phys. Letts. B206, 364 (1988)
- [11] S.D. Drell and A.C. Hearn, Phys. Rev. Lett. 16, 908 (1966)
- [12] S. Gerasimov, Sov. J. Nucl. Phys. 2, 930 (1966)
- [13] J.D. Bjorken, Phys. Rev. 148, 1467 (1966)
- [14] F.E. Close, in Reference [8]
- [15] I. Karliner, Phys. Rev. D7, 2717 (1973)